METIS: Final design of the Imager sub-system

Peter Bizenberger, Harald Baumeister, Jean-Christophe Barriere, Thomas Bertram, Armin Böhm, et al.

PROCEEDINGS OF SPIE

METIS: final design of the imager sub-system

Peter Bizenberger, Harald Baumeister, Jean-Christophe Barriere, Thomas Bertram, Armin Böhm, et al.

SPIE.

METIS: Final design of the Imager sub-system

Peter Bizenberger*[a], Harald Baumeister[a], Jean-Christophe Barriere[f], Thomas Bertram[a], Armin Böhm[a], Bernhard Brandl[g], M. Concepcion Cardenas Vazquez[a], Eduardo Chamorro[a], Markus Feldt[a], Adrian M. Glauser[d], Thomas Henning[a], Werner Laun[a], Dirk Lesman[b], Lars Mohr[a], Gert Raskin[e], Ralf-Rainer Rohloff[a], Silvia Scheithauer[a], Benoit Serra[h], Paula Stepien[a], Remko Stuik[g], Stephen Todd[c], Roy van Boekel[a]

[a]Max Planck Institute for Astronomy, Koenigstuhl 17, 69117 Heidelberg, Germany;
[b]NOVA, Dwingeloo, Netherlands, [c]STFC UKRI Edinburgh, United Kingdom, [d]ETH Zürich, Switzerland; [e]KUL Leuven, Belgium; [f]CEA Saclay, France; [g]Leiden Observatory, Netherlands; [h]ESO Garching, Germany

ABSTRACT

METIS, the Mid-infrared Imager and Spectrograph for the Extremely Large Telescope (ELT), is one of the three first-generation science instruments and about to complete its final design phase [1]. The Imager sub-system provides diffraction-limited imaging capabilities and low-resolution grism-spectroscopy in two channels: one covers the atmospheric L&M bands with a field of view of 11x11 arcsec, and the second covers the N band, with a field of view of 14x14 arcsec.

Both channels have a common collimator and a dichroic beam splitter dividing the light into two dedicated cameras and the corresponding detectors. In addition, the Imager provides a precise pupil re-imaging implementation allowing the positioning of high-contrast imaging masks for coronagraphic applications. The two channels are equipped with a HAWAII-2RG detector for LM-band and a GeoSnap detector for the N-band.

We present the final optical design of the Imager in a summary, as well as the cryo-mechanical concept. The mechanical design gives an overview of the general design aspects and the analyses that demonstrate the approach how to deal with demanding stability and alignment requirements for high-contrast imaging. It further focuses on the design of individual units as e.g., on the GeoSnap detector mount and on the pupil re-imager. In addition, we exemplarily outline some of the key alignment and verification tasks, essential to guarantee the performance of the Imager.

Keywords: ELT instruments, IR imaging, cryogenic optics, metal optics, mid-infrared, diffraction-limited optics, MAIT

1. INTRODUCTION

The light from the Extremely Large Telescope enters the METIS cryostat and passes the common fore optics (CFO), which provides image de-rotation and chopping capability, and passes into the Imager with a focal plane as optical interface.

The split between LM and N bands is done in the collimated section reflecting the longer wavelengths and transmitting the shorter ones. All three optical units are designed as a pure reflecting mirror design to cover the large wavelength range and to allow for a compact design to fit into the allocated space envelope of the cryostat. The two cameras are designed and optimized to match the dimensions given by the detector and to fulfil the requirements on field of view and sampling.

---

*biz@mpia.de   phone: +49 6221 528311   web: mpia.de

The Imager design is hierarchically built up by components, integrated into units, which again are integrated into assemblies. The three assemblies are designed with clear interfaces in order to allow an early and independent verification. These three assemblies are mounted to a backbone structure that allows a precise positioning of the optics and cryo-mechanical units. This backbone also supports all the interfaces for electrical housekeeping, cryogenic cooling, readout electronic high speed data link, mechanical mounting and the optical interface. The Imager is at a different temperature level than the rest of the METIS cryogenic sub-systems. This requires a complex interface to thermally isolate but also to allow a rigid and stable mechanical mounting. The mechanical interface to the fore optics acts as reference for the internal alignment in order to allow a simple integration at system level.
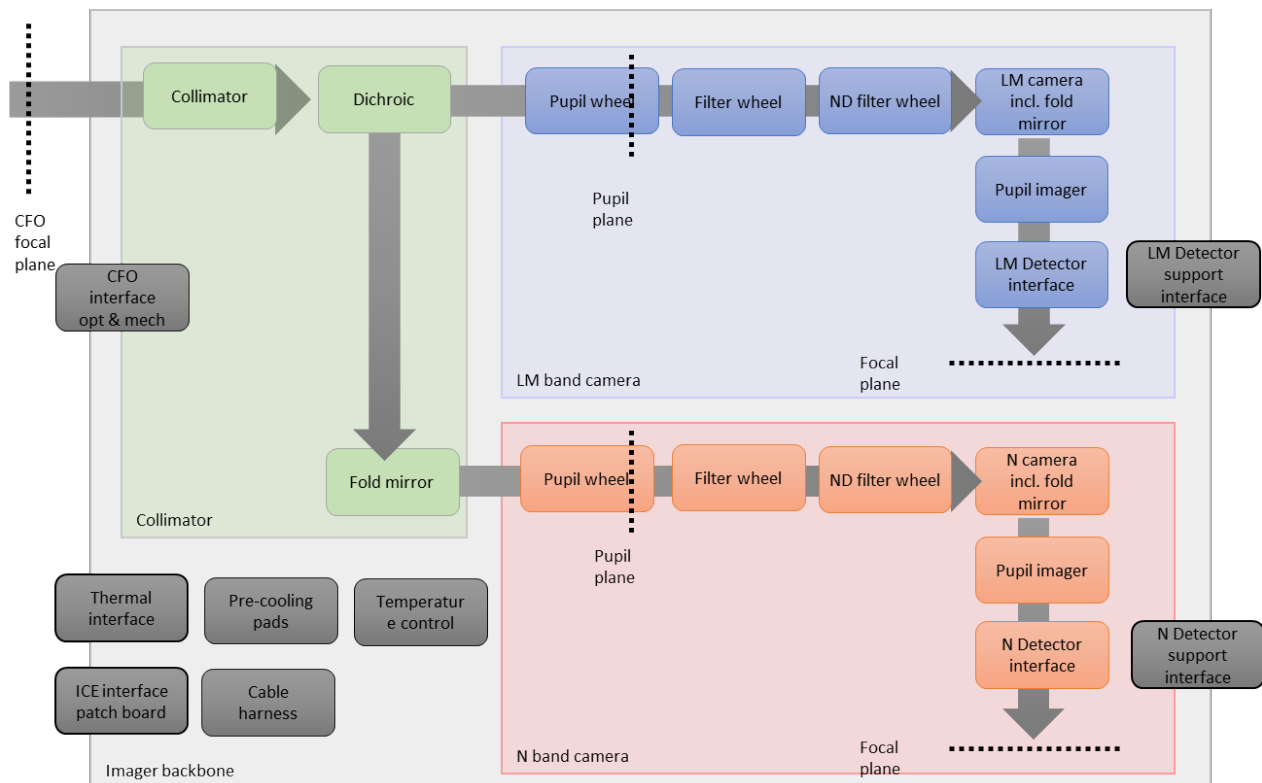

Figure 1. Conceptual layout of the METIS Imager. Three assemblies (collimator, LM band camera, and N band camera), mounted to a common backbone structure that incorporates all interfaces to other sub-systems.

The first assembly, in direction of light, is the collimator. It collimates the light and splits it into two separate channels. The split is upstream of the pupil, which allows the positioning of wavelength matching science filters and dispersive elements for long slit spectroscopy. It also allows the use of high contrast imaging (HCI) elements as apodizing phase plates (APP) [5][7], Lyot stops, or other background suppressing masks.

The separated beams are folded into the corresponding camera assemblies, which comprises the camera optics but also the pupil wheel, filter wheel, neutral density filter wheel, pupil re-Imager mechanism and the detector unit. Since these components depend on the wavelength range, they belong from a functional point of view to the camera assemblies. All wheel units, six in total, are equipped with an ICAR drive [6] that allows precise and repeatable positioning of the individual elements.

The limited space envelope requires and leads to a compact design with nested wheel assemblies and folded optics as illustrated in Figure 2 and Figure 3.
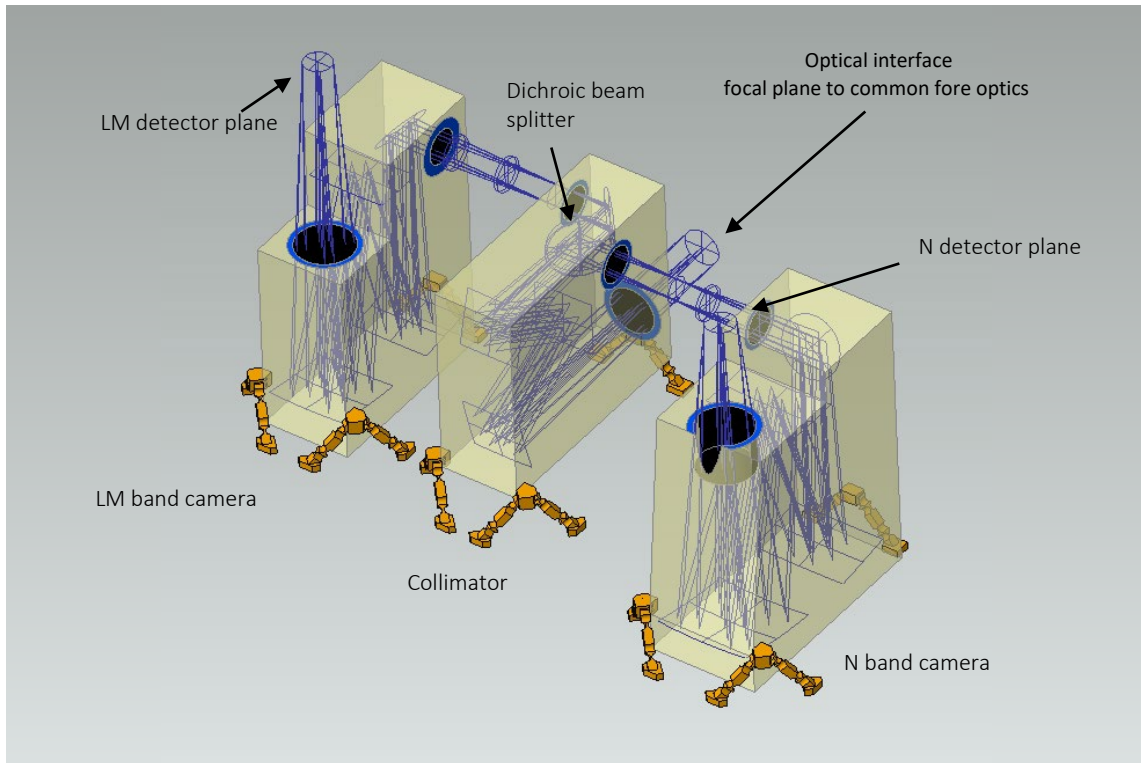
Figure 2: Opto-mechanical layout with 'black boxes' for optics representation. Optics mounted with bi-pods to the Imager backbone. Light enters horizontally with a focal plane as optical interface. The collimator is located in the centre, light is divided and folded into the two cameras.
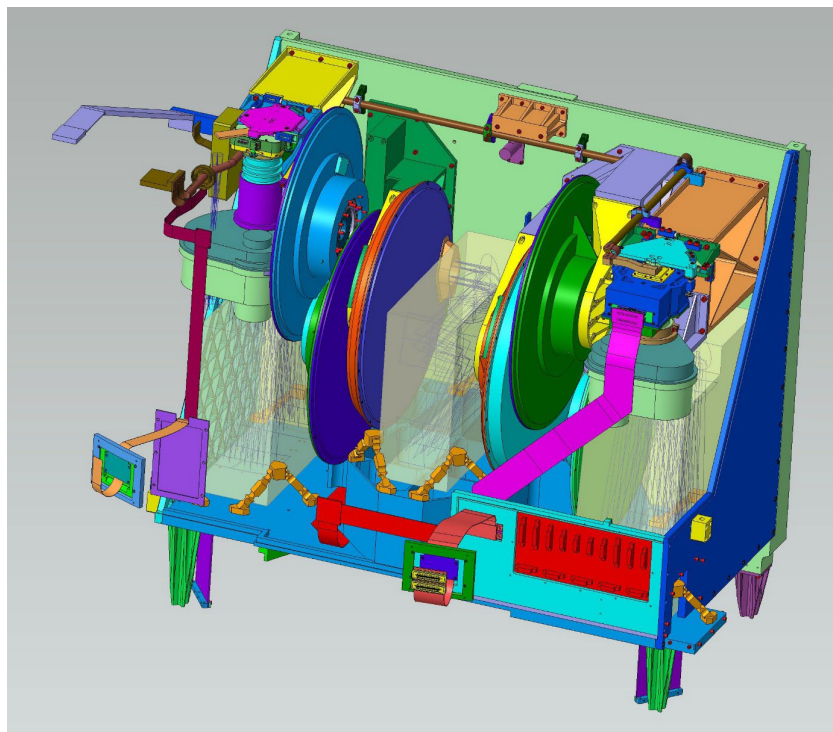

Figure 3: Complete view of the Imager sub-system, without the radiation shields. All unit interfaces are mounted to the L-shaped backbone structure.

2. OPTICAL DESIGN

The collimator and the two cameras are three-mirror anastigmat (TMA) systems. All surfaces are free-form mirrors, defined as Zernike surfaces with coefficients up to term 14. For manufacturing and in order to reduce the degrees of freedom to align, the M1 and M3 mirrors of the anastigmat are designed to share a common substrate. This approach allows for relative mechanical accuracy in the μm range.
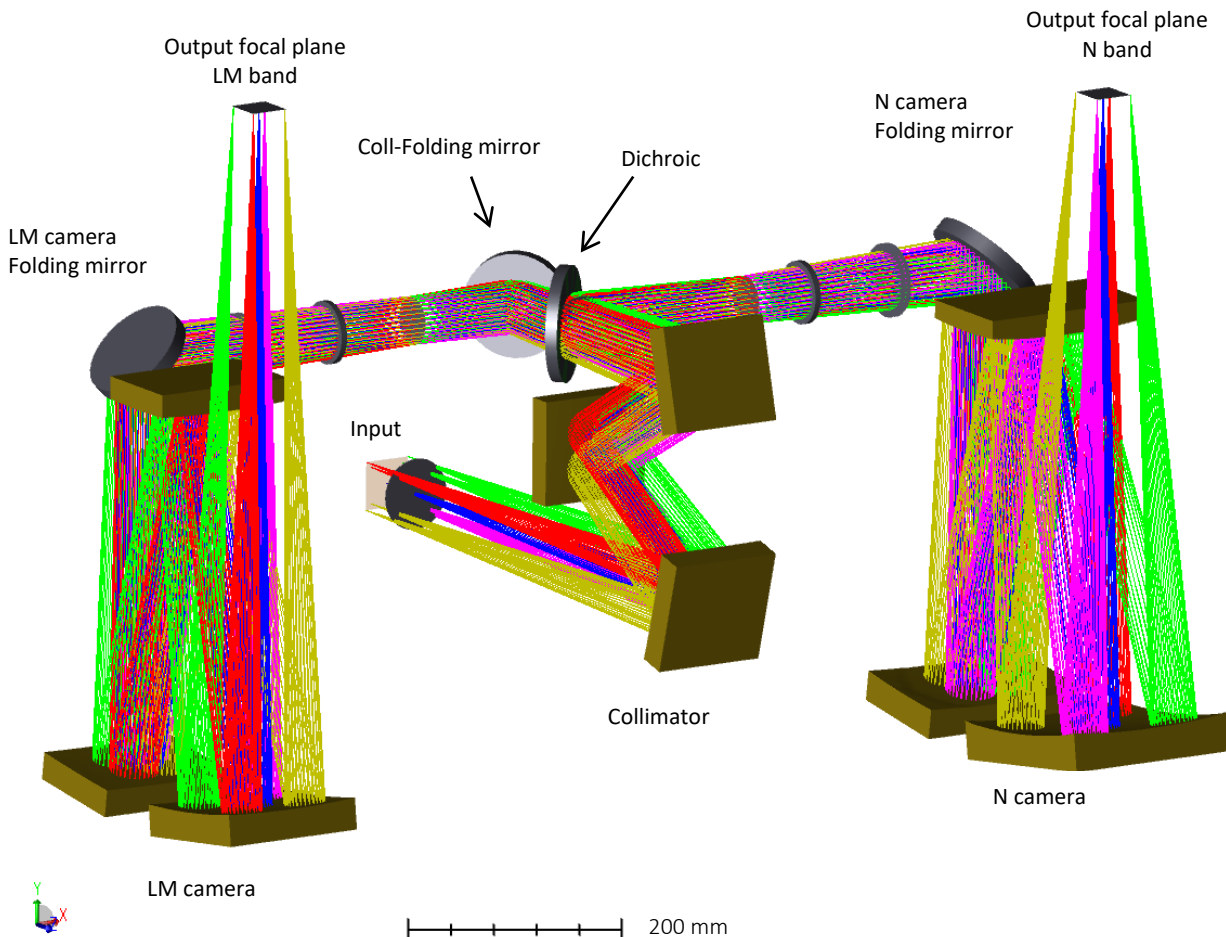

Figure 4: Layout of the Imager optics

2.1 Optical design considerations

The collimator is designed to serve both channels i.e., the complete wavelength range and the larger field of view for the N band detector. In addition, the collimator has the following design drivers which are derived from iterations with manufacturers and the alignment concept.

- The collimator focuses on the interface to the CFO. A certain front focal distance is required in order to allow free space for the kinematic mounting interface.
- The collimator forms the pupil of the Imager. This pupil must be real and accessible for mounting grisms, masks and HCI components. A certain back focus position is required and iterated with the mechanical design.
- The input and output axis of a TMA shall be parallel. This simplifies folding and alignment a lot.
- Slopes of the optical surfaces are constrained in order to match feasibility of the optics.
- Surface form is selected to be Zernike surface with coefficients up to term 14. Since these optics are manufactured as free form surfaces anyway, this allows some more degrees of freedom for optimization.

- The Zernike surfaces are used on-axis, but tilted, in order to allow clearance for the reflected beam.
- The collimator design shall deliver a collimated beam output, in order to place filters, grisms, etc. in the optical path without affecting the final performance. This approach also simplifies the alignment concept significantly.
- The total length and extension of the TMAs are limited and iterated with the mechanical design, in order to fit to the allocated envelope inside the cryostat.
- All optics are designed for an operating temperature of 40 Kelvin.
- The dichroic beam splitter is part of the collimator. Longer wavelengths (N band) shall be reflected, shorter wavelengths (LM band) transmitted. This allows a substrate transparent for alignment and verification at visible wavelength. For the nominal design of the collimator powered optics, the dichroic is initially not considered. This is valid since the collimator output shall be collimated.
- M1 and M3 are positioned such that they can be manufactured on one common support substrate. This reduces mechanical tolerances to the μm level. Thus, the complexity of the complete system alignment is reduced since there are less degrees of freedom to be controlled.
- The pupil diameter has been selected to be 45 mm, in accordance with feasibility for manufacturing, final dimension of the optics and mechanical design.
- Optimization shall be weighted for the on-axis field in order to achieve the best quality for HCI applications.
- Magnification is defined by the field of view requirement, detector size and pixel pitch.
- The image plane shall be perpendicular to the optical axis. This simplifies the integration and alignment of the detector.
- A long back focal distance for the cameras to provide space for pupil re-imaging lenses.

2.2 Basic layout of a TMA

The layout is chosen such that M1 and M3 of the TMA share a narrow common space envelope, which allows manufacturing on a common substrate. The appropriate constrains have been imposed during optimization of the system. The input and output axis are parallel, in order to allow a folding of the optics to fit inside the cryostat space envelope.
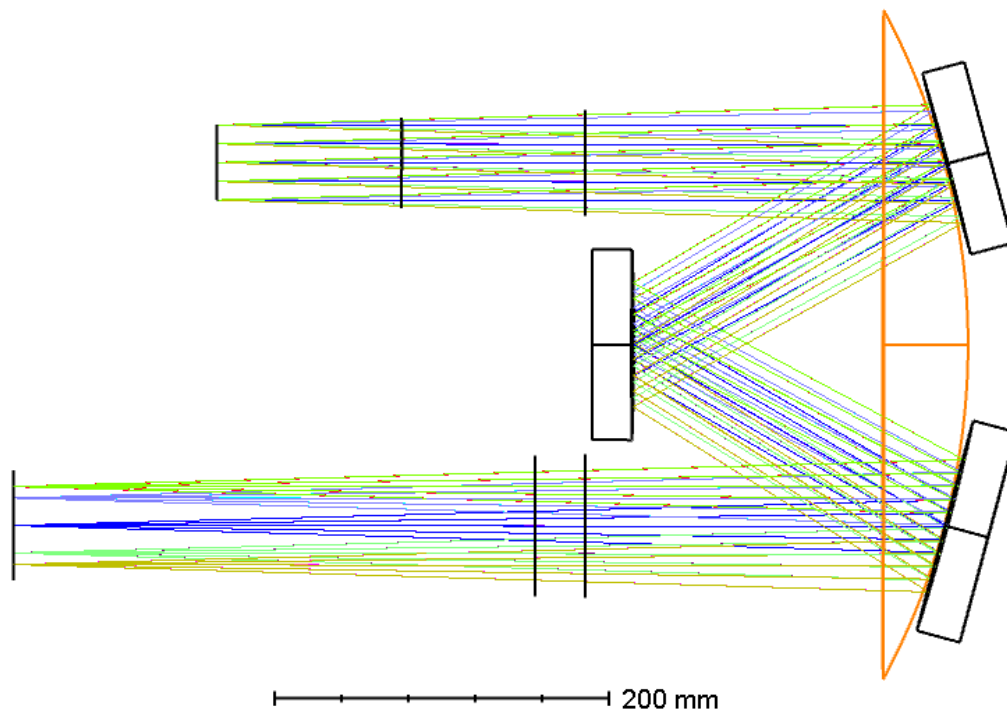

Figure 5: Basic concept of a TMA layout for all three optics of the Imager. M1 and M3 are within a certain envelope, matching a common radius.

2.3 Nominal performance

The design with Zernike surfaces for the mirror surfaces allows to address all the requirements listed in the previous section. The final end-to-end performance of the collimator and the camera leads to a well diffraction-limited optics that gives sufficient margin for manufacturing and alignment. An athermal design using identical material for housing and optics preserves the performance at cryogenic and ambient temperature [3]. The selection of pure, directly polished aluminium without any plating, prevents the bi-metallic effect. Several manufacturers are capable to produce mirrors in this technology with the requested accuracy for surface error and surface roughness.

Table 1: Nominal design wavefront error of the complete Imager optics.

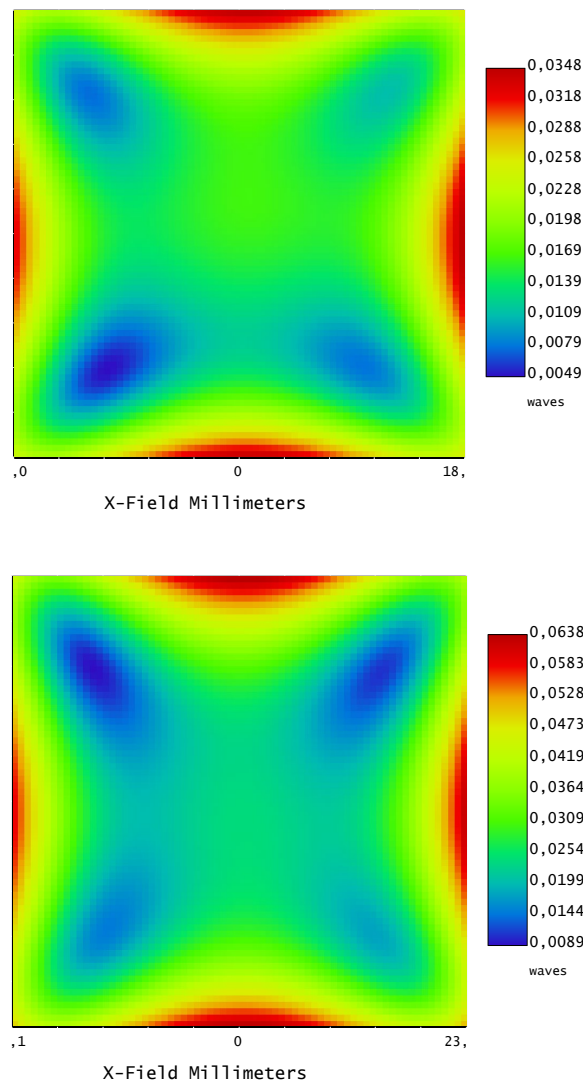| Item	Value
Wavefront error LM band, complete	24 nm RMS
Wavefront error N band, complete	44 nm RMS

Figure 6: Wavefront error map for the complete LM band channel (top) and N band channel (bottom). Reference wave for these plots is 1 μm to scale to RMS nm as unit.

2.4 Long slit spectroscopy

The Imager provides low resolution (R ≥ 200) slit spectroscopy covering the individual bands L, M and N, in one setting each. The dispersive elements are grisms that consist of a directly ruled grating on the second surface of the prism (prism's hypotenuse). The selected material for the grisms is germanium, with a maximum thickness of 10 mm. Both surfaces of the grisms will have an anti-reflex coating. The grisms are mounted to a motorized wheel that allows to switch between spectroscopy and imaging with pupil masks.
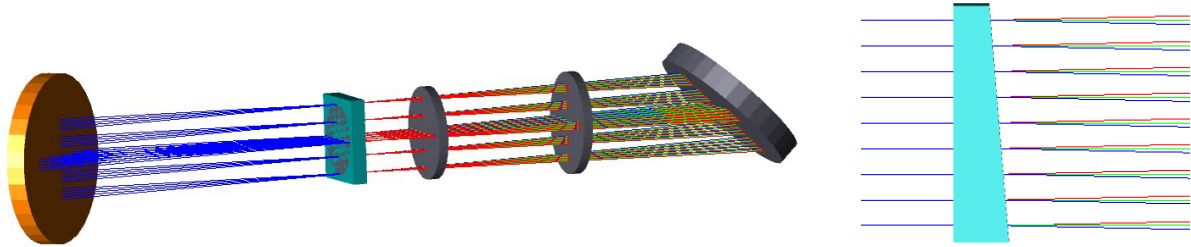

Figure 7: Setup with the grism in the pupil plane. Order sorting filters are placed behind the pupil.

Table 2: Grisms specification at operational conditions

Grism	Material	Central wavelength [µm]	Refraction index @ central wavelength @ working T, 40 K	Prism apex angle [deg]	Grating [lin/mm]	Max. Resolution with slit
L band	Germanium	3.55	3.9549	2.257	32.80	1476 (slit 63 µm)
M band	Germanium	4.85	3.9421	5.797	61.27	3786 (slit 63 µm)
N band	Germanium	10.50	3.9292	1.900	9.25	410 (slit 189 µm)

A set of slits with various widths is available for spectroscopy. Some of the slits are narrower than the PSF width of certain wavelengths. Diffraction effects and vignetting takes place at the slit itself and because of larger diffraction in one direction, also at the pupil stop. The total transmission loss depends on the slit width and the wavelength range defined by the selected order sorting filter.

The transmission has been calculated using physical optics propagation in OpticStudio. The selection of a narrow slit might increase the spectral resolution but reduces transmission.

3. CRYO-MECHANICAL DESIGN

In this section we focus on the mechanical design of the backbone structure and its corresponding analysis.
The backbone of the Imager is housing the wheel units, the detector units and the optics. This structure has references machined in one clamping to provide high accuracy positions for the alignment. Radiation shields and the thermal interface as well as the electrical patch board are also attached to the backbone structure.
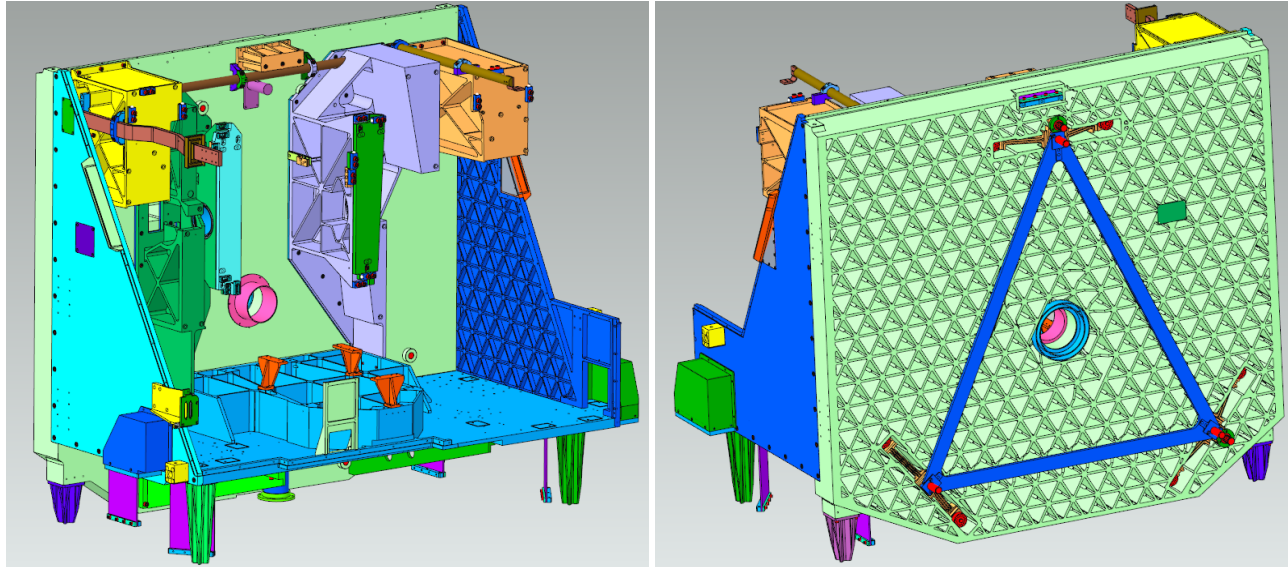

Figure 8: The Imager backbone with mounting structure for optics, wheel units and detector units (left). The vertical plate incorporates the bi-pod interface for mechanical mounting (right). In the middle, the clear through for the optical path is centred to the 3-point interface. This will also be used as reference for alignment of the optics, particularly for focus relative to the mechanical interface.

Figure 9: Super-bolt to fix the bi-pod interface

The backbone has a mechanical interface to mount the Imager to the common fore optics. Since these two sub-systems are at a different temperature level, 40 K versus 70 K, the interface must thermally separate those. It also must fulfil earthquake requirements, which is essential for operation in Chile. Main purpose is to support the optics, detector and wheel units with a precise tolerance.
The mechanical interface is realized by Titanium bi-pods, to guarantee thermal isolation and stability. Extended finite element analysis shows the expected performance and allows to optimize design issues. To avoid, e.g., torque into the spacers that would increase the force load, so called super-bolts are used to apply the required force for earthquake handling but not to stress the bi-pods.

A light-tight radiation shield cooled to 40 K is not shown in the previous pictures but also attached to the backbone structure.

In the following sections we present exemplarily the detector unit and the pupil re-Imager unit. Other units as filter wheel units or pupil wheel units are not addressed here.
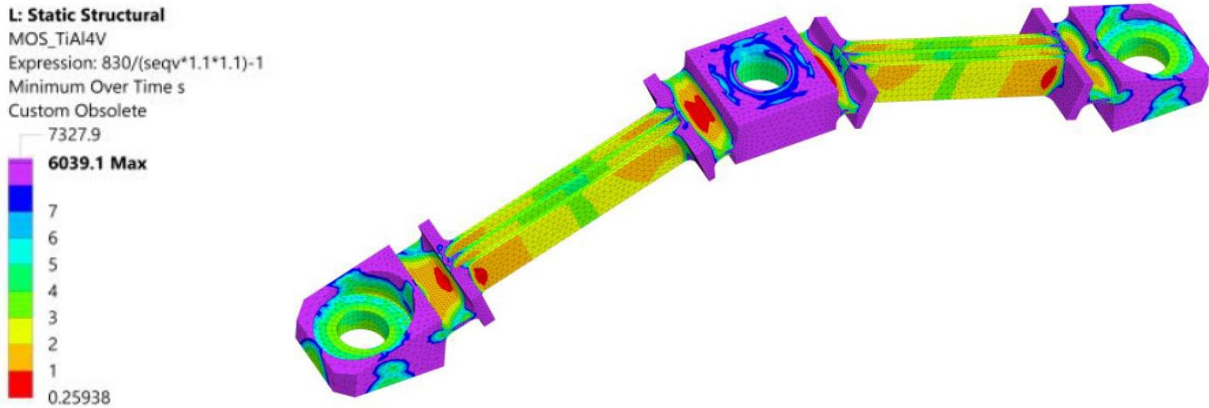
Figure 10: Finite element analysis of the titanium bi-pods that interface the METIS common fore optics. Temperature difference in the worst case between ambient and 40 K, and earthquake survival must be guaranteed.

4. DETECTOR UNIT

The Imager is equipped with a new Teledyne GeoSnap readout circuit [2] with a HgCdTe mid IR sensitive detector layer. The mount of this detector challenges the design in terms of electronics and mechanics. The fast data rate of 12.8 Gbit/s and the introduced stress due to cool down of materials with different coefficients of thermal expansion (CTE) needs to be addressed.
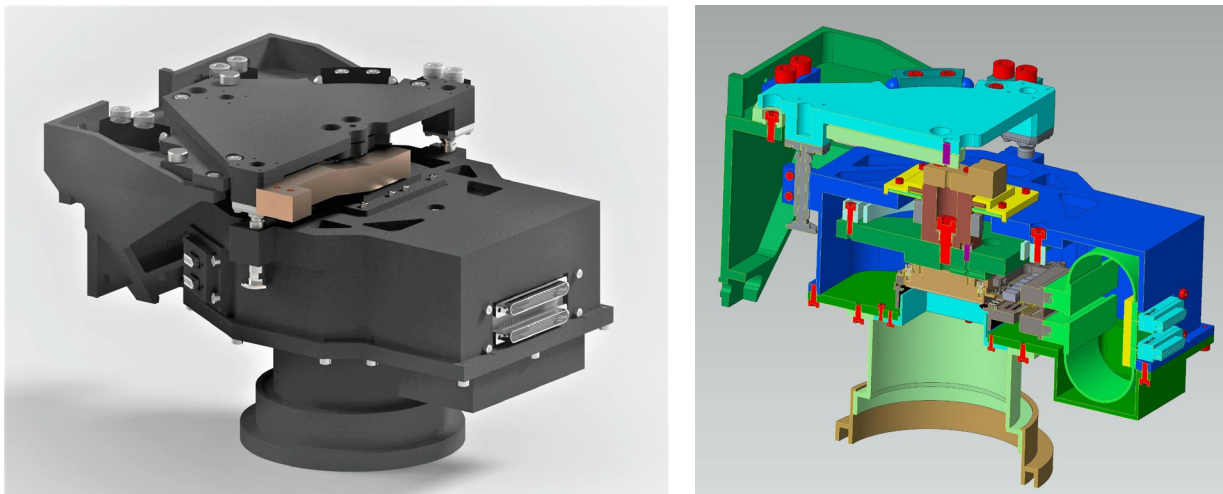

Figure 11: Mechanical design of the GeoSnap detector mount (left) and cross-section to illustrate the various components as titanium spacer ring, high speed cable extension, detector carrier, cooling connection, as well as the alignment features for lateral, rotation and focus adjustment.

To guarantee the survival of the detector during cool down, the different CTE values of the various components must be considered and differential shrinking compensated. This is taken in account with a titanium spacer ring, mounted to the aluminium housing and the molybdenum detector interface. Finite element analysis demonstrates the thermal behaviour in terms of heat conduction and introduced stress. The design is radial symmetric to avoid lateral shifts during cool down.
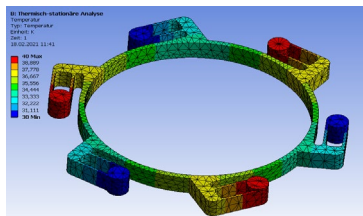
Figure 12: Analysis for titanium spacer ring. Three mounting 'ears' for the aluminium interface and three for the molybdenum interface of the detector.

The required high speed data rate challenges the design of the cryogenic cables, particularly for the vacuum feedthrough. Usually, the vacuum feedthrough is realized with hermetic military connectors. For these data rates, the available, but still custom-made connectors are extremely expensive and suffer from a long lead time. An alternative solution is foreseen for the Imager, to use sealed flex board feedthroughs, which are commercially available and are tested for functionality e.g., from Douglas Electrical.
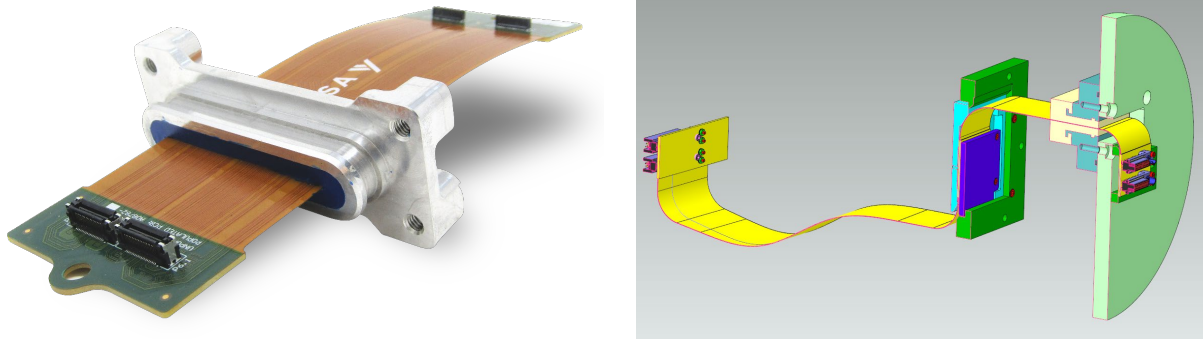

Figure 13: Vacuum feedthrough for high-speed flex boards (photo credit: Douglas Electric, https://blog.douglaselectrical.com/technology-blog), left. Cryogenic cable routing with thermal clamping and vacuum feedthrough, right.

5. PUPIL RE-IMAGER UNIT

The main science case for METIS is high-contrast imaging, realized with coronagraphic masks to cancel out the bright star light level. To achieve the required accuracy, well aligned pupils are essential to suppress photons leaking from the cancelled star. To align the pupil in the optical path, a pupil steering mirror is available in the common fore optics. The measurement of the pupil positions is done with a re-imaging optics that can be inserted into the optical path, just before the detector. In this setup, all upstream pupils can be imaged and analysed for co-alignment.

The design of the pupil re-imaging unit takes advantage and experience of previous instruments and well proven technology for cryogenic motor drives and cryogenic lens mounting [3][4].

The optical design is limited to a certain filter i.e., to one narrow band filter for each wavelength band. The optics consist of two air spaced lenses, one of ZnSe and one of ZnS. One surface is designed as toroidal surface for compensating the non-radial symmetric TMA design of the camera optics. Both re-Imager lenses, for LM channel and N channel, are very similar but not identical.

The lenses are mounted in 40° chamfers and are axial pre-loaded with spring washers. This allows CTE mismatch of lens material and aluminium mounts to be compensated for while maintaining lateral alignment free from play. This concept has already been used for many cryogenic instruments in the past [8][9]. The axial shift of the lenses due to cool down can be calculated and pre-set in the 'ambient' manufacturing drawings.

The drive is realized with a Phytron stepper motor and a Harmonic Drive gear (grey in Figure 14), both specified for cryogenic conditions.

The pupil re-Imager has two positions, in the beam and completely out of the beam. The required accuracy for the lateral position is very relaxed, the image of the pupils only gets shifted on the detector but does not suffer from image quality degradation.
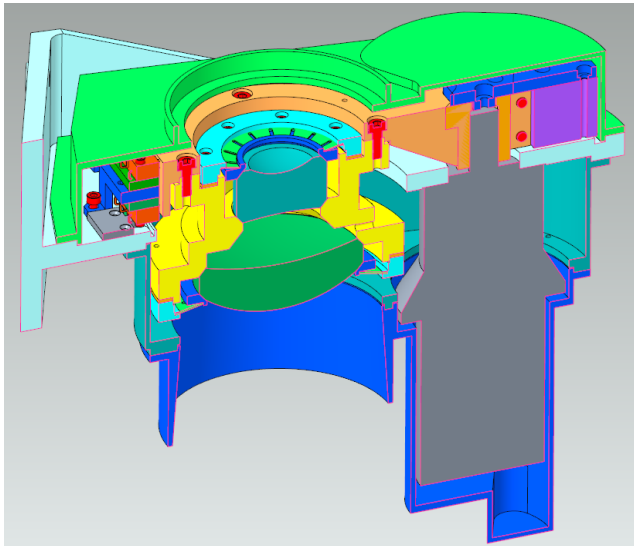
Figure 14: Cross section through the pupil re-Imager unit. Lenses (green) with wide chamfers. Cryogenic stepper motor and Harmonic Drive gear for positioning.

6. ALIGNMENT & VERIFICATION

The alignment and verification of performance for a complex and also compact instrument as the Imager requires a suitable AIV panning and effort. The AIV phase consists of more than 50 individual tasks, mainly at cryogenic, to align the system and verify the performance. These AIV tasks make use of a dedicated test cryostat, especially designed for the METIS Imager.

Some AIV-tasks can be executed in a smaller cryostat, which is available for cryogenic testing e.g., for interferometric measurements.

Figure 15: Lab setup of a cryostat that allows cryogenic measurements e.g., with auto-collimation telescope (left) or interferometer (right).

The final end-to-end verification of the Imager will take place in a test cryostat that mimics the real METIS interfaces for cooling and mechanical mounting. Identical coolers as in the final instrument are used to reach the temperature level of 40 K. The optical interface is materialized with alignment targets and masks. For the wavefront error verification and for aligning focus of the collimator, a reference ball is mounted to the mechanical interface of the backbone.
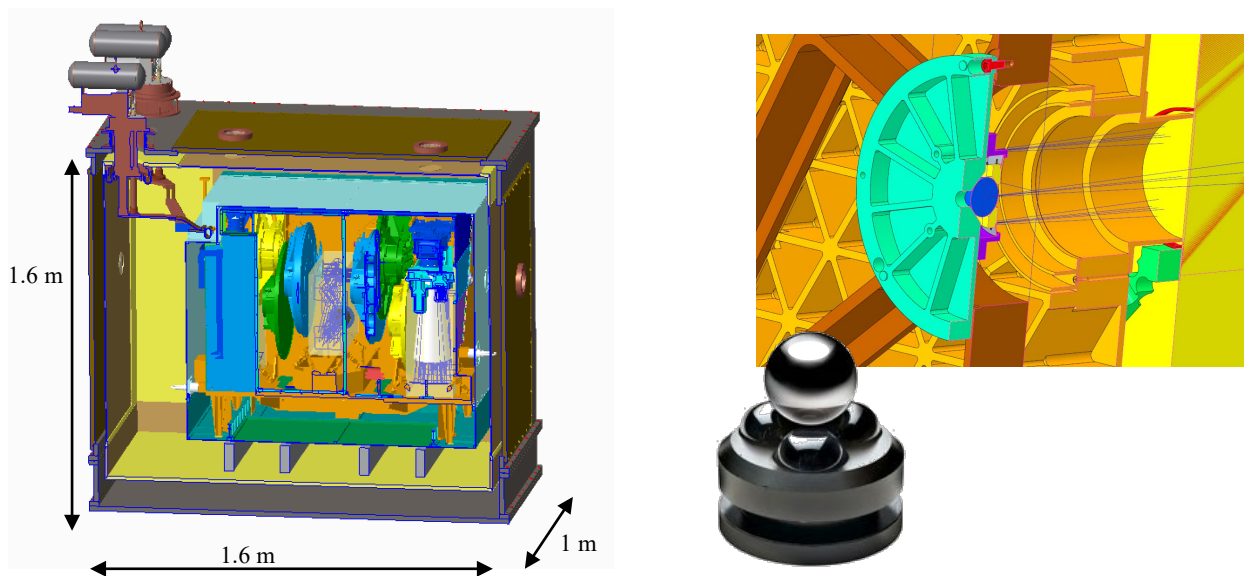

Figure 16: Imager test cryostat for final end to end verification (left). Reference ball for alignment of focus (right).

REFERENCES

[1] Brandl, B., et al., "Status of the Mid-IR ELT Imager and Spectrograph (METIS)", Ground-based and Airborn Instrumentation for Astronomy, VII, Proc of SPIE Vol. 10702 2018

[2] Jerram P., Beletic J., "Teledyne's high performance infrared detectors for Space missions", Proc. of SPIE Vol. 11180 International Conference on Space Optics, Chania, Greece 2018

[3] Bizenberger P, et al., "LINC-NIRVANA: Diffraction limited optics in cryogenic environment", Proc of SPIE 9147, Ground-based and Airborne Instrumentation for Astronomy V, Montreal 2014

[4] Baumeister H., Bizenberger P., Bailer-Jones C., Kovacs Z., Röser H., Rohloff R., "Cryogenic Engineering for Omega2000: Design and Performance", Proc. SPIE. 4841, Instrument Design and Performance for Optical/Infrared Ground-based Telescopes, Hawaii 2002

[5] Kenworthy M.A., Absil O., Carlomagno B., Agócs T., Por E. H., Brandl B., Snik F., "A review of high contrast imaging modes for METIS", Proc. SPIE 10702, Paper 10702-369 (2018)

[6] Barriere, J.-C., et al., "Qualification and performances of a highly repeatable cryogenic actuator", Proc of SPIE 10706-44 Advances in Optical and Mechanical Technologies for Telescopes and Instrumentation III, Austin, USA, 2018

[7] Snellen, I., de Kok, R., Birkby, J. L., Brandl, B., Brogi, M., Keller, C., Kenworthy, M., Schwarz, H., Stuik, R., "Combining high-dispersion spectroscopy with high contrast imaging: Probing rocky planets around our nearest neighbors", Astronomy & Astrophysics, Volume 576, A59 (2015)

[8] Bizenberger P., et al. "Optical design and cryogenic mounting of the optics for a pyramid waterfront sensor working in the near infrared wavelength range". In: vol. 5962. Proc. SPIE. Sept. 2005, pp. 674–684. DOI: 10.1117/12.639285

[9] Cárdenas Vázquez M. C. et al. "PANIC: A General-purpose Panoramic Near-infrared Camera for the Calar Alto Observatory". In: *PASP* 130 (Feb. 2018), p. 025003. DOI: 10.1088/1538-3873/aa9884